Linear combination of atomic orbitals calculation of the Auger neutralization rate of He^+ on Al(111), (100), and (110) surfaces

Diego Valdés,[1,*] E. C. Goldberg,[2] J. M. Blanco,[1] and R. C. Monreal[1]
[1]*Departamento de Física Teórica de la Materia Condensada, Universidad Autónoma de Madrid, E-28049 Madrid, Spain*
[2]*Instituto de Desarrollo Tecnológico para la Industria Química (CONICET-UNL), Güemes 3450, CC91, 3000-Santa Fe, Argentina*
(Received 14 March 2005; published 30 June 2005)

We develop a theory of the Auger neutralization rate of ions on solid surfaces in which the matrix elements for the transition are calculated by means of a linear combination of atomic orbitals technique. We apply the theory to the calculation of the Auger rate of He^+ on unreconstructed Al(111), (100), and (110) surfaces, assuming He^+ to approach these surfaces on high symmetry positions and compare them with the results of the jellium model. Although there are substantial differences between the Auger rates calculated with both kinds of approaches, those differences tend to compensate when evaluating the integral along the ion trajectory and, consequently, are of minor influence in some physical magnitudes like the ion survival probability for perpendicular energies larger than 100 eV. We find that many atoms contribute to the Auger process and small effects of lateral corrugation are registered.

DOI: 10.1103/PhysRevB.71.245417 PACS number(s): 79.20.Rf, 61.85.+p, 79.60.Bm

I. INTRODUCTION

Electron transfer between an ion or molecule and a surface proceeds via resonant and Auger processes. Resonant processes are basically one-electron processes that occur when one electron can tunnel to/from the energy level of the ion from/to the continuum of states in the solid. In contrast, Auger processes involve at least two electrons: the electron-electron Coulomb interaction causes the scattering of one electron of the solid to the ion while another electron is scattered from an occupied to an unoccupied state of the solid. The difficulty of dealing with an electron-electron interaction in a many-electron system has been the main cause why realistic theoretical calculations of the Auger neutralization rate of an ion in front of a metal surface have not been possible until recently. To our knowledge, all of these calculations have been performed by describing the metal surface within the jellium model,[1–7] focusing on the effect of collective excitations[1–5] and on ion-induced effects.[6,7] Very recently, precise measurements of the very small surviving scattered ion fractions of the He^+ in glancing collisions with Ag(111)[8,9] and Ag(110)[9] surfaces have revealed strong differences in the Auger neutralization probability of He^+ at these surfaces. The only way in which a jellium can model different crystallographic faces of the same metal is to withdraw the jellium edge from the first atomic layer by half an interplanar spacing.[10] In this way, good agreement between theory and experiment was achieved for He^+/Ag in Ref. 9. The dependence of the ion-survival probability of He^+ on Ag(110) has also been measured as a function of the azimuthal angle revealing strong differences between the two simmetry directions ([111] and [110]) along the surface and random directions.[11] Then, while a jelliumlike description of the Auger neutralization process has the appealing property of self-consistency, a more realistic description of the metal surface is needed to account for crystal effects.

The purpose of this work is to calculate Auger neutralization rates by going beyond the jellium model while still keeping the problem on relatively simple and computational feasible bounds. The atomic nature of the metal surface is taken into account by describing the electron that neutralizes the ion in a linear combination of atomic orbitals (LCAO) basis. This procedure has been applied to the calculation of energy levels and hopping interactions relevant for analyzing resonant processes.[7,12–15] A similar approach has been used to study resonant transition rates in Refs. 16 and 17. However, the metallic excitations accompanying the neutralization process will be still calculated by means of the response function of a jellium surface. The basic idea is to describe appropriately the "local" environment seen by the ion when it is neutralized even though we neglect band structure effects in the dielectric response of the metal to the neutralizing event. In Sec. II we present the theory. Calculations have been performed for He^+/Al in order to compare the results with the very good jelliumlike calculations existing for this system. This is done in Sec. III and in Sec. IV we present our conclusions. Atomic units ($e=\hbar=m=1$) are used throughout this work.

II. THEORY

Our starting point is the formula for the Auger neutralization rate of an ion in front of a solid, as given in linear response theory:[2,3]

$$\frac{1}{\tau}(\vec{R}_a) = 2\sum_{\vec{k},n}\int_0^\infty d\omega \int \frac{d^2\vec{q}_\parallel}{(2\pi)^2}\int_{-\infty}^{\infty} dz_1 \int_{-\infty}^{\infty} dz_2 \\ -\mathrm{Im}\,\chi(\vec{q}_\parallel,\omega;z_1,z_2)V_{\vec{k},n}(\vec{q}_\parallel,z_1)V^*_{\vec{k},n}(\vec{q}_\parallel,z_2) \\ \times\delta(\omega+E_a-\epsilon_{\vec{k},n}), \quad (1)$$

where

$$V_{\vec{k},n}(\vec{q}_\parallel,z) = \frac{2\pi}{q_\parallel}\langle\varphi_a(\vec{r}'-\vec{R}_a)|e^{i\vec{q}_\parallel\cdot\vec{\rho}'}e^{-q_\parallel|z-z'|}|\varphi_{\vec{k},n}(\vec{r}')\rangle. \quad (2)$$

In Eqs. (1) and (2), φ_a is the wave function of the atomic orbital of energy E_a for an ion at the position $\vec{R}_a$, $\varphi_{\vec{k},n}$ is the wave function of a Bloch electron in the solid with wave vector $\vec{k}$ in the band n of energy $\epsilon_{\vec{k},n}$, and $\chi(\vec{q}_\parallel,\omega;z_1,z_2)$ is the screened susceptibility of the solid, Fourier transformed in the coordinates parallel to the surface which then depends on the perpendicular coordinates z_1 and z_2. The sum in Eq. (1) is over occupied states and the δ function expresses energy conservation in the Auger process. Also it is assumed that the ion velocity is much smaller than the Fermi velocity of the metal electrons: the Auger rate is independent of velocity in this case and can be calculated assuming the ion to be at rest. The reason for this is purely kinematic: in the reference frame where the ion is at rest, the metal electrons move with velocities $v_e=v_F\pm v$, where v_F is the Fermi velocity and v is the ion velocity. Consequently, $v_e\approx v_F$ for $v\ll v_F$ and the process happens as if the ion where at rest. The formula for the Auger transition rate can be written for an arbitrary parallel velocity by means of a displacement of the Fermi sphere, but the calculation becomes more involved. In this work we will restrict to the simplest case $v\ll v_F$.

In previous calculations of the Auger neutralization rate, the jellium model was used in the evaluation of the screened susceptibility and the matrix elements of Eq. (2) as well. The requirement that wave functions have to be orthogonal was taken into account by using the orthogonalized plane wave (OPW) method, in which $\varphi_{\vec{k}}$ is taken as a plane wave made orthogonal to the ion state φ_a.[18] In this work we follow a different approach and take φ_{kn} as a Bloch state written in a linear combination of atomic orbitals (LCAO) basis:

$$\varphi_{\vec{k},n}(\vec{r})=\frac{1}{\sqrt{N}}\sum_\alpha C_\alpha^{(n)}(\vec{k})\sum_{\vec{R}} e^{i\vec{k}\cdot\vec{R}}\varphi_\alpha(\vec{r}-\vec{R}), \tag{3}$$

where $\varphi_\alpha(\vec{r}-\vec{R})$ is the wave function of the α orbital of the atom of the solid placed at the lattice position $\vec{R}$, N is the number of cells in the crystal, and the coefficientes $C_\alpha^{(n)}(\vec{k})$ give rise to the band structure. Then, the matrix elements of Eq. (2) can be expressed as linear combinations of matrix elements for atomic orbitals as

$$V_{\vec{k},n}(\vec{q}_\parallel,z)=\frac{1}{\sqrt{N}}\sum_\alpha C_\alpha^{(n)}(\vec{k})\sum_{\vec{R}} e^{i\vec{k}\cdot\vec{R}}V_{\alpha,\vec{R}}(\vec{q}_\parallel,z), \tag{4}$$

with

$$V_{\alpha,\vec{R}}(\vec{q}_\parallel,z)=\frac{2\pi}{q_\parallel}\langle\varphi_a(\vec{r}'-\vec{R}_a)|e^{i\vec{q}_\parallel\cdot\vec{\rho}'}e^{-q_\parallel|z-z'|}|\varphi_\alpha(\vec{r}'-\vec{R})\rangle. \tag{5}$$

Substituting Eq. (4) into Eq. (1) and making use of the identity,

$$\sum_{\vec{k},n}\int_0^\infty d\omega\,\delta(\omega+E_a-\epsilon_{\vec{k},n}) = \sum_{\vec{k},n}\delta(\epsilon-\epsilon_{\vec{k},n})\int_0^\infty d\omega\,\delta(\omega+E_a-\epsilon), \tag{6}$$

Eq. (1) is written down as

$$\frac{1}{\tau}(\vec{R}_a)=2\sum_{\alpha,\vec{R}}\sum_{\alpha',\vec{R}'}\int_0^\infty d\omega\,\delta(\omega+E_a-\epsilon)\rho_{\alpha\vec{R};\alpha'\vec{R}'}(\epsilon) \times\int\frac{d^2\vec{q}_\parallel}{(2\pi)^2}\int_{-\infty}^\infty dz_1\int_{-\infty}^\infty dz_2 -\mathrm{Im}\,\chi(\vec{q}_\parallel,\omega;z_1,z_2)V_{\alpha,\vec{R}}(\vec{q}_\parallel,z_1)V^*_{\alpha',\vec{R}'}(\vec{q}_\parallel,z_2), \tag{7}$$

where $\rho_{\alpha\vec{R};\alpha'\vec{R}'}(\epsilon)$ is the density of states of the unperturbed surface expressed in the basis $\{\alpha\vec{R}\}$ of localized states. Notice in Eq. (7) that energy conservation prevents electrons in bands having energies below E_a (such as core-electron levels) to contribute directly to the Auger process.

When calculating the matrix elements $V_{\alpha,\vec{R}}(\vec{q}_\parallel,z)$ according to Eq. (5) we follow the procedure of Refs. 12–15 and use an orthonormal basis of *Löwdin's* wave functions

$$\varphi_\mu=\sum_\nu (S^{-1/2})_{\mu\nu}\psi_\nu, \tag{8}$$

ψ_ν being the atomic wave function associated with the ν orbital and $S_{\mu\nu}=\langle\psi_\mu|\psi_\nu\rangle$ the overlap. In this way we include in the calculation of the Auger neutralization rate the hybridization between ion and solid, which is known to be very important when studying resonant processes between ions and metals. In our approach, we start with a set of atomic orbitals ψ_ν as obtained from Hartree-Fock calculations for Al and He atoms.[19] We include all the occupied orbitals of Al (K and L shells and the $3s$ and $3p$ orbitals of the M shell) and the $1s$ orbital of He. Then we construct the *Löwdin's* basis as indicated by Eq. (8) and the orthogonal orbitals φ_μ are the ones to be introduced in Eq. (5). We consider that the band structure of the Al surfaces will not be affected by the presence of He and therefore density of states are calculated for unperturbed and unreconstructed Al surfaces using the tight-binding parameters of Ref. 20 and the FIREBALL code of Ref. 21. Finally, the electronic excitations accompanying the neutralization process will be described by the susceptibility of a jellium surface. The screening properties of a metal surface, including the possibility of sustaining collective excitations, can be most easily described within the jellium model. We will apply this model to Al, which is the prototype of a free-electron metal. In particular, in this work $\chi(\vec{q}_\parallel,\omega;z_1,z_2)$ is calculated for a jellium confined by a step-potential barrier model, with the height of the barrier $W=E_F+\phi$, E_F being the Fermi energy and ϕ the work function.[2] It was shown in Ref. 4 that this is a reasonable approximation when compared with the susceptibility calculated with the difuse Lang-Kohn barrier.

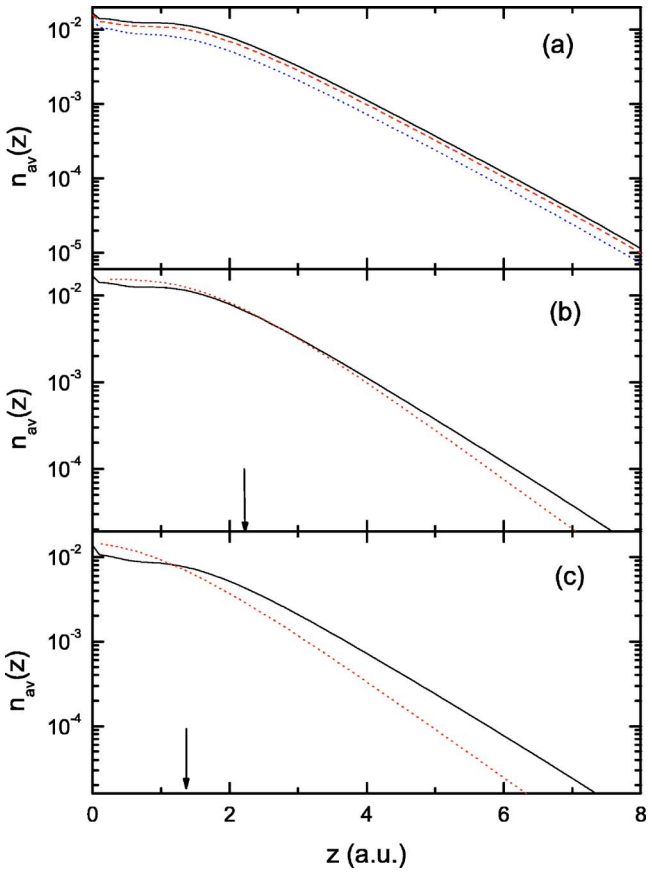

FIG. 1. (Color online) (a) Valence-electron density, averaged in the coordinates parallel to the surface over a unit cell, for: Al(111) (continuous line), (100) (dashed line), and (110) (dotted line) surfaces. (b) The averaged valence-electron density of Al(111) (continuous line) is compared with the electron density obtained for a jellium of $r_s=2$ a.u. confined by a Lang-Kohn potential barrier (dotted line). The jellium edge is marked by an arrow on the z axis. (c) The same as in (b) but for the Al(110) surface. All densities are plotted as a function of the distance to the first atomic layer.

III. RESULTS

In this section we present results for the Auger neutralization rate of He^+ on unreconstructed Al(111), (110), and (100) surfaces and compare them with the results obtained using the jellium model. It will be relevant for the following discussion to look first at the electronic densities of these unperturbed surfaces as calculated with the LCAO method and with the jellium model. This gives us a rough idea of how symilarly the wave functions of electrons are described by both methods. In Fig. 1(a) we show the electronic density (per spin) of Al(111), (110), and (100) surfaces, obtained from the valence $3s$ and $3p$ orbitals of Al, averaged over a unit cell in the coordinates parallel to the surface as a function of the distance to the first atomic layer. We observe that the close-packed (111) surface has the biggest density and the open (110) surface the smallest density at every distance. Then we expect the Auger neutralization probability of He^+ to be the largest at the (111) surface and the smallest at the (110) surface, since the Auger neutralization rate is roughly proportional to the electronic density. In Figs. 1(b) and 1(c) the averaged densities for Al(111) and (110) surfaces are compared to the electronic density of the jellium model. For the jellium calculation we use a Lang-Kohn potential barrier for $r_s=2$ a.u.,[10] with the jellium edge withdrawn by half of the interplanar distance d_p, $\frac{1}{2}d_p=2.21$ a.u. for Al(111) in Fig. 1(b) and $\frac{1}{2}d_p=1.35$ a.u. for Al (110) in Fig. 1(c). We notice in Fig. 1(b) that the jellium model with the jellium edge withdrawn by $\frac{1}{2}d_p$ with respect to the first atomic layer is a good approximation to the LCAO density of the Al(111) surface while for the open (110) surface of Fig. 1(c) the agreement is not as good, the jellium density being much smaller than the LCAO density for distances larger than 2 a.u. from the first atomic layer.

Next we present results for the Auger neutralization rate. For simplicity, in this work we will assume that He approaches the surface perpendicularly on a high symmetry position with respect to a surface unit cell, either on top of an atom of Al of the first layer (on-top position) or in the center of the surface unit cell (hollow position). Therefore the results of the present calculation will be pertinent only for experiments done in normal incidence and with velocities small in comparison with the Fermi velocity of Al, since our Auger rate is calculated in this approximation. Distance z is perpendicular to the surface and measured with respect to the first atomic layer. The energy level of He in front of Al should depend on the distance to the surface and on the relative position of the ion with respect to the surface unit cell as well, but a calculation of energy level variations is outside the scope of this work. Therefore most of the results presented here have been obtained by keeping the energy level of He fixed at −22.6 eV with respect to the vacuum level: this means that we have assumed a constant upward shift of 2 eV. It turns out that 2 eV is a remarkable universal figure for He^+ neutralizing on a variety of solid surfaces.[22] This will be justified at the end of this section by comparing calculations of the Auger rate done with the distance-dependent energy level of He of Ref. 22 and with a constant energy level shifted up by 2 eV.

In Fig. 2 we compare the Auger neutralization rate of He^+ on Al(111), (100), and (110) surfaces as a function of the distance to the first atomic layer assuming that He^+ approaches Al on-top position. We find differences between the three surfaces, the Auger rate following the behavior of the electronic density of Fig. 1(a). Notice that the slope of the rate is the same for the three surfaces. This justifies the assumption made in Ref. 9 that the Auger neutralization rate of He^+ on Ag(111) and Ag(110) has the same exponential decrease with distance.

The relevant results for the Auger neutralization rates that we will present next can be understood by looking at the overlap between He and Al. Figure 3 shows the overlap integrals between the He-$1s$ and the s and p_z orbitals of each shell of Al. Notice that for distances larger than 2 a.u. only the $3s$ and $3p_z$ valence orbitals of Al have a non-negligible overlap with He. In this range of distances both overlaps decrease exponentially, while for distances smaller than 2 a.u. the overlap between He-$1s$ and the Al-$3s$ orbitals tends to saturate and the one between the He-$1s$ and Al-$3p_z$ orbitals decreases strongly. On the other hand, the Al-core orbitals have an overlap with He comparable to that of the Al-

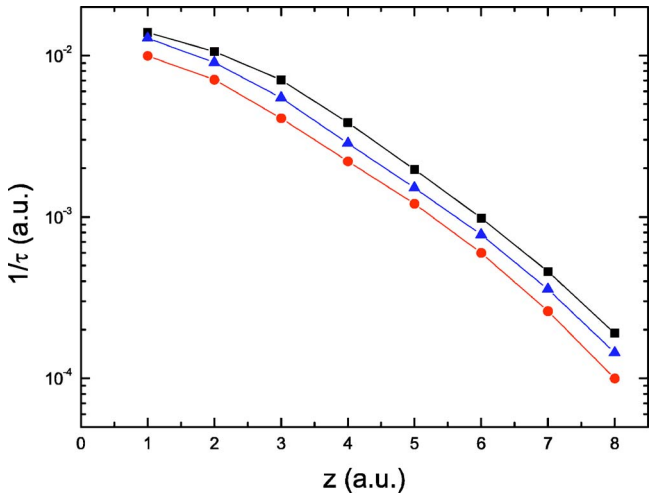

FIG. 2. (Color online) The Auger neutralization rate of He^+ on Al(111) (squares), (100) (triangles), and (110) (dots) surfaces as a function of distance to the first atomic layer. He^+ is assumed to approach these surfaces on-top position.

valence orbitals only for distances smaller than 1 a.u. Also notice that the decay of the overlap between the He-1s and the Al-3p_z orbitals is rather slow: it decreases one order of magnitude in 6 a.u. of distance.

Figure 4 compares the Auger neutralization rate of He^+ on Al(111) calculated with the LCAO method and with the jellium model. We show results for He approaching the surface on the following symmetry positions: on-top and on the two nonequivalent hollow positions labeled 1 and 2 in the figure. Notice that, while the LCAO calculation gives results rather independent of the position with respect to the surface unit cell, they are very different from the jellium calculation. This is surprising because we have seen in Fig. 1 that both kinds of calculations produce nearly the same electronic density for the unperturbed Al surface: the differences seen in electronic density do not justify the large differences in the Auger rates. Therefore the reason for the discrepancy can only be due to

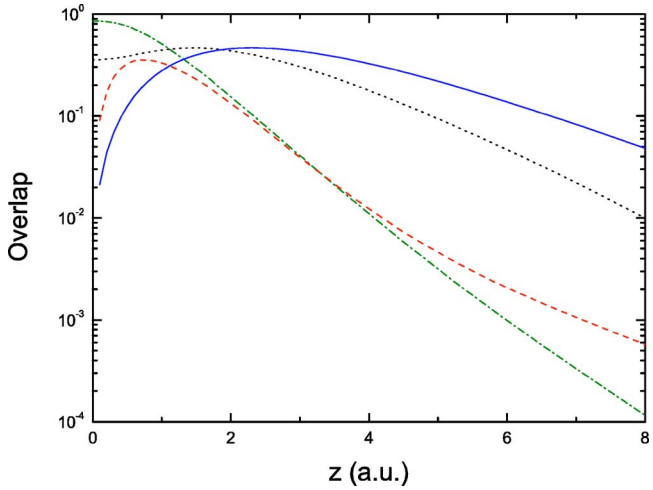

FIG. 3. (Color online) Overlap between He-1s and the following orbitals of Al: 2s (single dot, dashed line), 2p_z (dashed line), 3s (dotted line), and 3p_z (continous line).

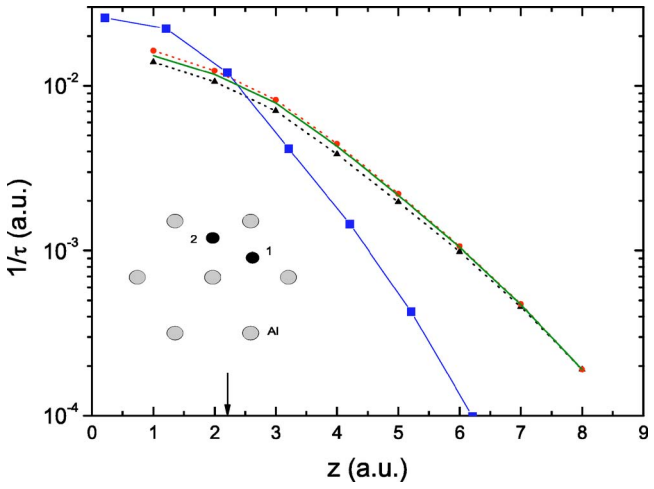

FIG. 4. (Color online) The Auger neutralization rate of He^+ approaching perpendicularly the Al(111) surface at the lateral positions shown in the inset: on-top (triangles, dotted line), hollow 1 (dots, dotted line), and hollow 2 (solid line without symbols). The Auger rate calculated using the jellium model is also shown (squares, solid line). Distance is measured with respect to the first atomic layer. The jellium edge is marked by an arrow on the z axis.

the different way in which both methods describe hybridization between He and Al: OPW method versus *Löwdin's* orbitals. The orders-of-magnitude differences between the jellium and LCAO calculations at large distances are of little consequence for Auger neutralization because of the very small values of the neutralization probabilities at these distances. The important region is where neutralization takes place and this is near the jellium edge.[7–9] Interestingly, the jellium and LCAO curves cross within this region and this will tend to wash-out the differences, as we will discuss below. An important point is that the Al-1s, 2s, and 2p core-orbitals play no role in the Auger neutralization of He^+ on Al, since we obtain virtually no change in the values of the Auger rate when we withdraw them from the calculation. This was to be expected from the small values of their overlap with He, shown in Fig. 3. We should point out that the core-orbitals enter in the calculation only through the orthogonalization procedure because, as we discussed after Eq. (7), their direct contribution to Auger neutralization is forbiden by energy conservation.

The insensitiveness of the Auger rate to the lateral position of the He within the surface unit cell suggests that many atoms contribute to the process. To see that this is true, we neglect in our Eq. (7) all the terms having $\vec{R}' \neq \vec{R}$, in which case the Auger rate can be written down as a sum of contributions of atoms placed at different lattice points. The results for the Al(111) surface with He-on top position are shown in Fig. 5. Notice in this figure how the contribution of the Al atom directly on top of He decreases for distances smaller than 2 a.u., consistently with the decrease in overlap shown in Fig. 3. Then, first and second neighbors on the first atomic layer give the most important contribution at short distances while they contribute as much as the Al-on top atom at large distances, due to the slow decay of overlap with distance shown in Fig. 3 and the high coordination number of the fcc

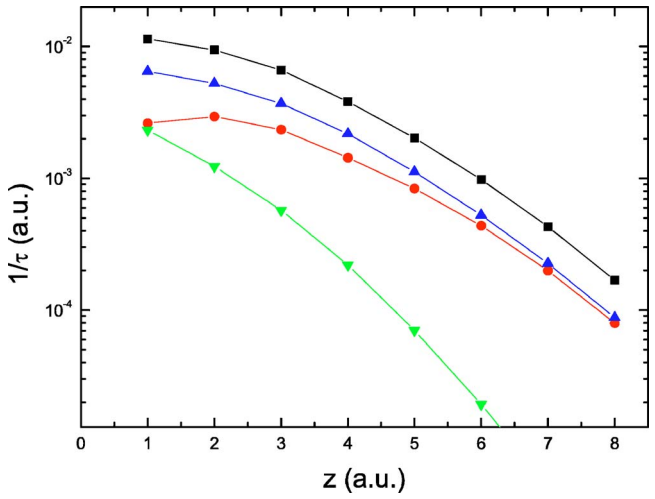

FIG. 5. (Color online) Contribution of different neighbors to the Auger neutralization rate of He^+ on Al(111). The total result (squares) is the sum of: the Al atom on-top of He (dots), its first and second neighbors in the first atomic layer (triangles up), and its first and second neighbors in the second atomic layer (triangles down). Other atoms give negligible contribution.

(111) surface. Atoms in the second atomic layer do not contribute much to Auger neutralization except at very close distances.

Figure 6 compares the Auger rate of He^+ approaching the Al(110) surface on-top position and on the central hollow position. There is essentially no difference between the two positions at large distances, like in the Al(111) case, due to the slow decrease of overlap with distance, but at short distances the hollow position gives a larger rate than the on-top position. This is again the consequence of the decrease in overlap between He and Al-$3p_z$ at distances smaller than 2 a.u. In Fig. 7 we present the contributions of atoms in

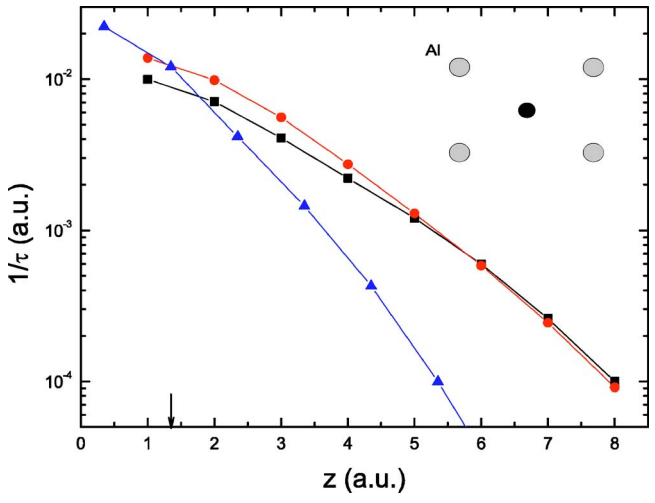

FIG. 6. (Color online) The Auger neutralization rate of He^+ approaching perpendicularly the Al(110) surface at the lateral positions shown in the inset: on-top (squares) and hollow (dots). The Auger rate calculated using the jellium model is also shown (triangles). Distance is measured with respect to the first atomic layer. The jellium edge is marked by an arrow on the z axis.

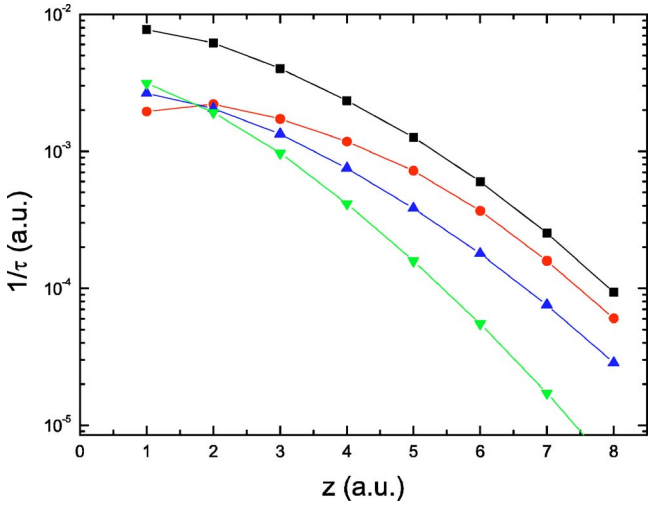

FIG. 7. (Color online) Contribution of different neighbors to the Auger neutralization rate of He^+ on Al(110). The total result (squares) is the sum of: the Al atom on-top of He (dots), its first, second, and third neighbors in the first atomic layer (triangles up) and in the second atomic layer (triangles down). Other atoms give negligible contribution.

different atomic layers to the Auger rate of He^+ on Al(110). In this case the Al atom on-top of He gives the most important contribution at large distances due to the low coordination of this surface but, for distances smaller than 2 a.u., even the second layer gives one-third of the value of the rate. We should mention that the result labeled total in this figure and the one in Fig. 6 do not correspond to the same calculation because in the former case we have neglected the crossed terms in Eq. (7). Even if these terms are always smaller than the direct ones, their contributions cannot be neglected in general since they can increase the Auger rate by 10%.

Next we discuss effects of energy level variation in the Auger neutralization rate of He^+ on Al. In Fig. 8 we show the diabatic and adiabatic energy levels of He approaching Al(111) on- top position. The diabatic level is taken from Ref. 23. The adiabatic level is obtained as the peak of the spectral density of states produced when the hoppings interactions of Ref. 23 between the diabatic He level and the Al levels are introduced as explained in Ref. 24. This adiabatic He level is the one we need to calculate the Auger neutralization rate because we know that the Auger process takes place at this energy level at low velocities.[24] At large distances, the level shifts up in energy due to the image interaction and at distances of about 5 a.u. the hopping interaction with the valence 3s and 3p orbitals of Al sets in, making the level go down in energy. Finally, at distances smaller than 2 a.u., the hopping interaction with the core levels 2s and 2p of Al causes the quick promotion of the He-1s level shown in the figure. In Fig. 9 we compare the Auger rate of He^+ on Al(111) calculated using the final adiabatic He-1s level of Fig. 8, with the calculation in which the level is shifted up in energy by a constant amount of 2 eV. Note how insensitive the Auger rate is to the actual values of the energy level except for very close distances, when the level crosses the bottom of the conduction band. Therefore to calculate

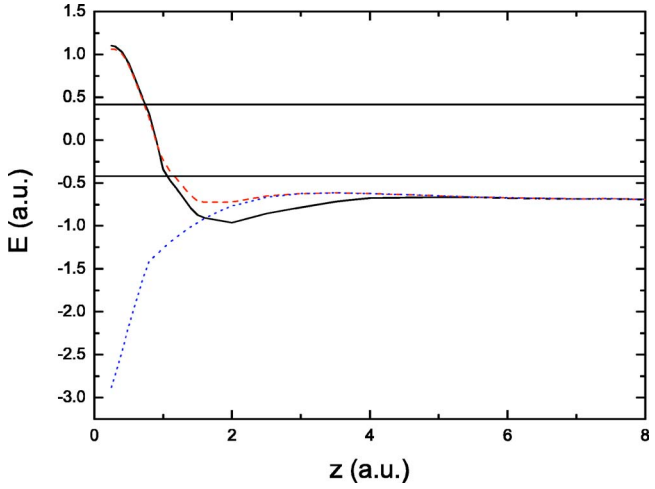

FIG. 8. (Color online) Energy levels (with respect to the Fermi level) for He^+ approaching the Al(111) surface on-top position. Dotted line: diabatic level. Dashed line: adiabatic level due to the interaction with the core electrons of Al. Continous line: final adiabatic level due to the interaction of He with all the electrons of Al. The top and the bottom of the conduction band are marked by two horizontal lines.

Auger neutralization rates assuming a constant value of the He-1*s* level will be an excellent approximation except when He gets closer than 1.4 a.u. of an Al atom. This is because, as we said before, the promotion of the He level is due to the hopping interaction with the core levels of Al and this interaction is appreciable only for He—Al interatomic distances smaller than 1.5–2.0 a.u., as shown in Fig. 8.

Figure 10 summarizes how the main results presented so far for the Auger transition rates influence ion survival probabilities. The ion survival probability is calculated as

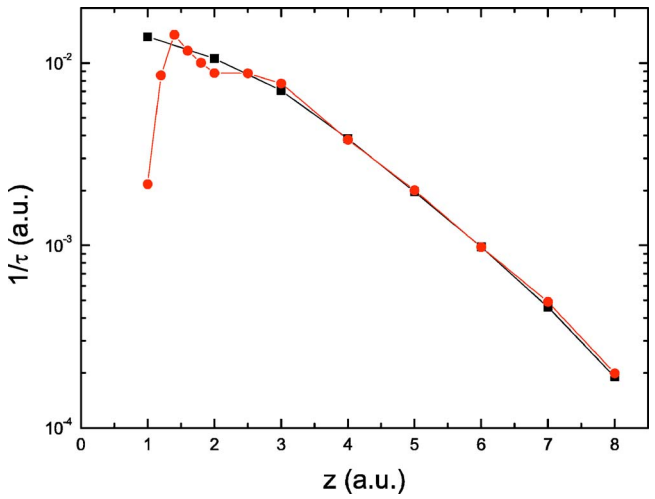

FIG. 9. (Color online) The Auger neutralization rate of He^+ on Al(111) using the final adiabatic energy level in Fig. 8 (dots) is compared with the calculation in which the level is shifted up by a constant amount of 2 eV (squares).

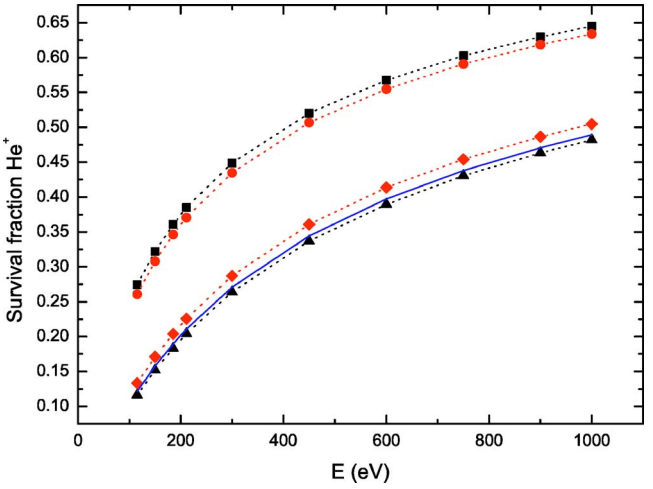

FIG. 10. (Color online) Survival fraction of He^+ in perpendicular incidence and with a scattering angle of 180° vs incident energy. For the (110) surface we show results using the calculated Auger neutralization rates with the LCAO (dots, dotted line) and the jellium models (squares, dotted line), using a distance-independent He-1*s* level. The same for the (111) surface is shown by the solid line without symbols and triangles up, respectively. Results for the (111) surface, using the distance-dependent final adiabatic level of Fig. 8 are shown as diamonds, dotted line.

$$P^+ = \exp\left\{-\left(\frac{1}{v_{in}} + \frac{1}{v_{out}}\right)\int_{z_s}^{\infty}\frac{dz}{\tau(z)}\right\}, \tag{9}$$

where v_{in} and v_{out} are the perpendicular velocities in the incident and outgoing trajectories and z_s the turning point. In Fig. 10 we show calculations of the Auger survival probability of He^+ on Al(111) and (110) surfaces at normal incidence, as a function of the incident energy. He^+ is assumed to be scattered off an Al atom of the first atomic layer with a scattering angle of 180° and, for simplicity, the turning points of all the trajectories are set to 1 a.u. We first notice that the jellium and the LCAO calculations presented here give similar ion survival probabilities for the Al(111) and (110) cases in spite of the differences shown by the Auger rates in Figs. 4 and 6, respectively. This can be understood from the above-mentioned crossing, near the jellium edge, of the values of $1/\tau$ calculated with jellium and LCAO models: the ion survival probability involves the integral of $1/\tau$ along the full trajectory and it turns out that both models produce the same "mean value" of $1/\tau$ in the region of distances around 2 a.u., where Auger neutralization occurs most probably. (A different situation may arise in resonant neutralization/ionization of an atomic energy level that crosses the de Fermi level at large distances, as is the case of Li^+ on Al analyzed in Ref. 16.) The differences between ion survival probabilities calculated with the two models should be larger for trajectories having turning points larger than 2 a.u. but those are only possible for the very small perpendicular energies attainable in grazing incidence experiments. In those experiments, however, also differences in $1/\tau$ with the position of He^+ with respect to the surface cell may play a role in giving the final value of the ion survival probability.

For comparison Fig. 10 also shows a calculation of the Auger survival probability that takes into account energy level variation and we see that these effects are negligible since energy level variation influences the Auger rate only in a rather small part of the full trajectory. We think that effects of energy level variation will be of little consequence in the Auger survival probability of He^+ scattering off the surface at grazing angles, as well. In this case, the distance of closest approach is usually larger than 1.5 a.u. as shown by calculated trajectories for He^+ scattering off Ag(111) and Ag(110) at random directions.[9] On the other hand, the parallel energy is large and consequently the time spent by He in close proximity of an Al atom is small in comparison with the time spent along the full trajectory. We get a rough estimation of the effect in the following way. Assume that He^+, with a parallel energy of 4 keV, would scatter on top of an Al atom at a distance of closest approach of 1 a.u. from it. Then the ion survival probability calculated by taking energy level variation into account will be less than 10% larger than the same probability calculated with a constant He-1*s* level.

IV. CONCLUSIONS

In this work we have calculated the Auger neutralization rate of He^+ on Al(111), (100), and (110) surfaces using a LCAO approach in the evaluation of the matrix elements for the transition. These calculations show that the Auger rate of the Al(111) surface is the largest and the one of the (110) surface the smallest, as suggested by the behavior of the electronic density. We find small differences in the Auger neutralization rate with lateral position of He with respect to the surface unit cell. This is due to the slow decrease with distance of the overlap between He and Al atoms that makes it possible for many Al atoms to contribute to the Auger process. The same conclusion has been reached in Ref. 16 for the resonant rates of Li^+ on Al(110). When compared with calculations of $1/\tau$ using the jellium model we find substantial differences. However, these differences should not be overestimated because both kinds of calculations give nearly the same result for measurable magnitudes that involve the integral of $1/\tau$ along the trajectory, such as the ion survival probability. In summary, the jellium model provides an excellent approximation for describing Auger neutralization of He^+ on Al. We are presently calculating Auger neutralization rates of He^+ on noble metal surfaces to investigate possible effects of band structure. Finally, another important conclusion of our work is that the variation of the energy level of He^+ in front of Al has little influence on the magnitude of the Auger neutralization rate, even though it determines the gain or loss of kinetic energy of He during the interaction process.

ACKNOWLEDGMENT

This work has been funded by the Spanish Comisión Interministerial de Ciencia y Tecnología under project BFM 2001-0150.

*Corresponding author. Fax: +34914974950. Email address: diego.valdes@uam.es

[1] T. Fonden and A. Zwartkruis, Phys. Rev. B **48**, 15603 (1993).
[2] R. Monreal and N. Lorente, Phys. Rev. B **52**, 4760 (1995).
[3] N. Lorente and R. Monreal, Phys. Rev. B **53**, 9622 (1996).
[4] N. Lorente and R. Monreal, Surf. Sci. **370**, 324 (1997).
[5] H. Jouin, F. A. Gutierrez, and C. Harel, Phys. Rev. A **63**, 052901 (2001).
[6] M. A. Cazalilla, N. Lorente, R. D. Muiño, J. P. Gauyacq, D. Teillet-Billy, and P. M. Echenique, Phys. Rev. B **58**, 13991 (1998).
[7] W. More, J. Merino, R. Monreal, P. Pou, and F. Flores, Phys. Rev. B **58**, 7385 (1998).
[8] S. Wethekam, A. Mertens, and H. Winter, Phys. Rev. Lett. **90**, 037602 (2003).
[9] Yu. Bandurin, V. A. Esaulov, L. Guillemot, and R. C. Monreal, Phys. Rev. Lett. **92**, 017601 (2004).
[10] N. D. Lang and W. Kohn, Phys. Rev. B **1**, 4555 (1970).
[11] Yu. Bandurin, V. A. Esaulov, L. Guillemot, and R. C. Monreal, Phys. Status Solidi B **241**, 2367 (2004).
[12] J. Merino, N. Lorente, W. More, F. Flores, and M. Yu. Gusev, Nucl. Instrum. Methods Phys. Res. B **125**, 250 (1997).
[13] J. Merino, N. Lorente, P. Pou, and F. Flores, Phys. Rev. B **54**, 10959 (1996).
[14] P. G. Bolcatto, E. C. Goldberg, and M. C. G. Passeggi, Phys. Rev. A **50**, 4643 (1994).
[15] J. O. Lugo, L. I. Vergara, P. G. Bolcatto, and E. C. Goldberg, Phys. Rev. A **65**, 022503 (2002).
[16] M. Taylor and P. Nordlander, Phys. Rev. B **64**, 115422 (2001).
[17] K. Niedfeldt, E. A. Carter, and P. Nordlander, J. Chem. Phys. **121**, 3751 (2004).
[18] P. M. Echenique, F. Flores, and R. M. Ritchie, in *Solid State Physics: Advances in Research and Applications*, edited by H. Ehrenreich and D. Turnbull (Academic, New York, 1990), Vol. 43, p. 229.
[19] S. Huzinaga, J. Chem. Phys. **42**, 1293 (1965).
[20] D. A. Papaconstantopoulos, *Handbook of the Band Structure of Elemental Solids* (Plenum Press, New York, 1986).
[21] P. Jelinek, H. Wang, J. P. Lewis, O. F. Sankey, and J. Ortega, Phys. Rev. B **71**, 235101 (2005).
[22] H. D. Hagstrum, Phys. Rev. **96**, 336 (1954).
[23] N. P. Wang, Evelina A. García, R. Monreal, F. Flores, E. C. Goldberg, H. H. Brongersma, and P. Bauer, Phys. Rev. A **64**, 012901 (2001).
[24] Evelina A. García, N. P. Wang, R. C. Monreal, and E. C. Goldberg, Phys. Rev. B **67**, 205426 (2003).